C. R. Chimie 18 (2015) 619–625

Contents lists available at ScienceDirect

Comptes Rendus Chimie

www.sciencedirect.com

Full paper/Mémoire

Synthesis, spectroscopic studies, thermal analyses, biological activity of tridentate-coordinated transition-metal complexes [M(L)X_2] and crystal structure of [ZnBr_2(2,6-bis(*tert*-butylthiomethyl)pyridine)]

Hanan F. AbdEl-Halim [a,*], Gehad G. Mohamed [b], Kathrin Hofmann [c], Barbara Albert [c]

[a] *Pharmaceutical Chemistry Department, Faculty of Pharmacy, Misr International University, Heliopolis, Cairo, Egypt*
[b] *Chemistry Department, Faculty of Science, Cairo University, 12613 Giza, Egypt*
[c] *Eduard-Zintl-Institute of Inorganic and Physical Chemistry, Technische Universität Darmstadt, Darmstadt, Germany*

ARTICLE INFO

Article history:
Received 15 September 2014
Accepted after revision 16 October 2014
Available online 14 April 2015

Keywords:
2,6-bis(*tert*-butylthiomethyl)pyridine
Metal complexes
Spectroscopy
Crystal structure
Biological activity

ABSTRACT

A new terdentate acyclic pincer ligand, 2,6-bis(*tert*-butylthiomethyl)pyridine (tbtmp), was synthesized and reacted with several complexes of iron, zinc, nickel, cobalt, and copper. The ligand and its coordination compounds were characterized using elemental analysis, infrared, ^{1}H- and ^{13}C-NMR-spectroscopy, thermal analyses, plus—for the Zn complex—single-crystal X-ray diffractometry. The structure of [Zn(L)Br_2] was solved in the tetragonal crystal system, chiral space groups $P4_12_12$ and $P4_32_12$ (No. 92 and No. 96, a = 947.2(1) pm, c = 2265.2(5) pm), revealing five-fold coordination of the metal atoms. According to spectroscopy, all complexes share the same coordination environment around the metal atoms, consisting of two halide anions and a sulfur-methylene-pyridine-methylene-sulfur entity; tbtmp acts as a tridentate ligand with the pyridine *N* atom and both *tert*-butylthio *S* atoms coordinating to the metal ions (NS2). The analysis results indicate that the metal ions are coordinated as distorted pseudo-bipyramids, LMX_2, with the chelate ligand meridionally arranged. One of the complexes contains ethanol as an additional ligand, resulting in a pseudo-octahedral coordination sphere [Ni(L)Cl_2EtOH]. The latter was obtained in the form of green crystals, which turn into a red powder with loss of the ethanol molecule. Fe (III), Co(II), Ni(II) and Cu(II) metal complexes [M(L)Cl_2] were screened for their antibacterial activity against *B. subtilis* G(+) and *Escherichia coli* G(−) bacteria, and fungus (*Candida albicans* and *Aspergillus flavus*).

1. Introduction

Transition-metal complexes that are coordinatively unsaturated may play an important role in catalytic processes. Thus, the synthesis of new complexes is highly desirable. Their reactivity can be used to functionalize simple organic molecules [1]. The stabilization of highly unsaturated intermediates in homogeneous catalysis may be attributed to agostic interactions of ligands with the metal [2]. It was observed that bulky phosphine ligands PR(*t*-Bu)$_2$ may stabilize unsaturated Ir(III) complexes by prohibiting dimerization and solvent coordination [3]. In previous studies concerning such complexes, it was explained that the ligands protect sterically the empty

* Corresponding author.
E-mail address: Hanan.Farouk2@yahoo.com (H.F. AbdEl-Halim).

http://dx.doi.org/10.1016/j.crci.2014.10.004
1631-0748/

coordination sites but do not interact directly beyond metal–phosphorus bonding. For many applications, pincer-type ligands were found to be important functional units, e.g., in catalysts [4–9] or sensors [10], as stabilizers of unstable cationic complexes [11], for molecular switches [12,13], and for the synthesis of supramolecular complexes and materials [14–18]. The pincer ligand class E′E2 (E with N, P or S donors and E′ that can be either a pyridine N- or a sp^2–type C-atom) has experienced a renaissance [19], since its earliest appearance in monometal coordination chemistry. Often, this ligand is found as a meridional ligand (i.e., E′ and E will be approximately coplanar in the metal coordination sphere). Barker et al. [20] reported a ligand with the pincer NS_2 functionalities and its complexes with Rh and Pd. Mononuclear complexes with a surrounding penta-coordinated metal atom were found in the crystal structures of [$ZnCl_2$(2,6bis((ethylthio)methyl)pyridine)] [21] and [$CuCl_2$(2,6bis((ethylthio)methyl) pyridine)][22]. For the dichlorocadmium(II) and analogous Co(II) complex [23], dinuclear structures and an octahedral arrangement were found. In 1998, the first Ru(II)–NS_2 complexes were reported [24], as well as related macrocyclic tridentate pyridine derivative NS_2 ligands [22]. Metallacyclopentadienyl derivatives have been studied kinetically, the mechanism reactions between pyridylthioether olefin Pd(0) substrates and substituted alkynes, the attack of the alkyne forming a reactive monoalkyne intermediate was found to be the rate-determining step in the case of less hindered ancillary ligands [25]. Also, three macrocyclic oxygen and NS_2-containing ligands and their Cu(II), Ni(II) and Co(II) complexes were synthesized before [26]. Pd(0) olefin complexes [Pd(η^2-olefin)(SNS)] and [Pd(η^2-olefin)(NSN)] have been reported. The intimate mechanism of olefin exchange involved a path promoted by the third dangling coordinating atom, which induces olefin dissociation and stabilizes the ensuing Pd(0) three-coordinated species [27].

In this work, 2,6-bis(*tert*-butylthiomethyl)pyridine and its Fe(II), Co(II), Ni(II), Cu(II) and Zn(II) complexes were prepared for the first time, hoping for a pronounced influence of the bulky alkyl group (*tert*-butyl) in the tridentate ligand. The ligand and its new transition-metal complexes were characterized by elemental analysis, IR, ^{1}H-, and ^{13}C-NMR spectroscopy. Crystal structure determination was possible for the Zn(II) complex. Thermal stability and biological activity were investigated for selected compounds.

2. Experimental

2.1. Materials

Unless specifically mentioned, all operations were performed under nitrogen atmosphere. Methanol was dried with metallic magnesium. The solvents were degassed in vacuo to eliminate oxygen. Sodium methoxide was prepared from sodium and methanol. 2,6-bis(bromomethyl) pyridine was prepared according to the reported procedure [28]. *t*-Butylthiol (Sigma) was used as purchased. The metal salts $CuCl_2{\cdot}2H_2O$ (Sigma), $CoCl_2{\cdot}3H_2O$, $NiCl_2{\cdot}6H_2O$ (BDH), $ZnBr_2{\cdot}4H_2O$ (Ubichem), and $FeCl_2{\cdot}2H_2O$ (Sigma) were used as purchased. All synthesized complexes melted above 300 °C.

Microanalysis was performed using Elemental Analyzer C.E. EA 1108. IR spectra were obtained on an FT-IR PerkinElmer 1740 spectrophotometer (KBr pellets), covering the range between 400 cm^{-1} and 4000 cm^{-1}. ^{1}H- and ^{13}C {^{1}H}-NMR spectra were recorded on a Bruker ARX-300 spectrometer ($CDCl_3$ solutions, tetramethylsilane was used as a standard).

2.2. Synthesis of 2,6-bis(tert-butylthiomethyl)pyridine (tbtmp)

tert-Butylthiol (2.3 cm^3, 20.38 mmol) was added to a stirred solution of sodium (0.54 g, 20.38 mmol) in methanol (25 cm^3). The mixture was stirred for a further 30 minutes and then added to a solution of 2,6-bis(bromomethyl) pyridine (2.7 g, 10.19 mmol) in methanol (50 cm^3). After heating under reflux (3 h) and cooling to room temperature, methanol was evaporated under reduced pressure. The resulting deep yellow residue was extracted with diethyl ether (150 cm^3) and the organic layer was washed twice with aqueous Na_2CO_3 solution (2 × 100 cm^3), dried over $MgSO_4$ and in vacuo. The resulting solid was slightly yellow, yield: 2.57 g (89%). FT-IR: ν(C = N), ν_{sym}(C–S), δ_{sym}(C–S) and ν_{asym}(C–S) are 1589, 1163, 993 and 750 cm^{-1}, respectively. ^{1}H-NMR: δ = 7.58 (t, 3J(H,H) = 6.40 Hz, 1H, py), 7.29 (d, 3J(H,H) = 6.85 Hz, 2H, py), 3.91 (s, 4H, -CH_2-S) and 1.34 ppm (s, 18H,–$C(CH_3)_3$). ^{13}C {^{1}H}-NMR: δ = 158.65 (s, C1, py), 136.99 (s, C3, py), 121.52 (s, C2, py), 43.09 (s,–S–C (CH_3)$_3$), 35.55 (s,–CH_2–S) and 30.99 ppm (s,–$C(CH_3)_3$). Anal. calcd for $C_{15}H_{25}NS_2$: C, 63.55; H, 8.89; N, 4.94; S, 22.62. Found: C, 63.12; H, 8.87; N, 4.95; S, 22.18.

2.3. Synthesis of [$FeCl_2$(2,6-bis(tert-butylthiomethyl)pyridine)]

$FeCl_2{\cdot}2H_2O$ (179.5 mg, 1.413 mmol) in ethanol (5 cm^3) was added to tbtmp (400 mg, 1.413 mmol) in ethanol (10 cm^3). After reacting for 30 minutes at room temperature, a yellow solid was precipitated. It was filtered, washed with ethanol and dried under vacuum. Yield: 0.26 g (36%). FT-IR: ν(C = N), ν_{sym}(C–S), δ_{sym}(C–S), ν_{asym}(C–S), ν(M–N) and ν(M–S) are 1599, 1161, 883, 763, 565 and 457 cm^{-1}, respectively. Anal. calcd for [$FeCl_2(C_{15}H_{25}NS_2)$]: C, 43.92; H, 6.14; N, 3.41; S, 15.63. Found: C, 43.40; H, 6.19; N, 3.37; S, 15.14.

2.4. Synthesis of [$CoCl_2$(2,6-bis(tert-butylthiomethyl)pyridine)]

The blue compound was obtained from $CoCl_2{\cdot}3H_2O$ (183.7 mg, 1.413 mmol) as described above. Yield: 0.35 g (86%). FT-IR: ν(C=N), ν_{sym}(C–S), δ_{sym}(C–S), ν_{asym}(C–S), ν(M-N) and ν(M–S) are 1600, 1161, 883, 713, 575 and 430 cm^{-1}, respectively. Anal. calcd for [$CoCl_2(C_{15}H_{25}NS_2)$]: C, 43.59; H, 6.10; N, 3.39; S, 15.52. Found: C, 43.23; H, 6.11; N, 3.29; S, 15.30.

2.5. Synthesis of [$NiCl_2$(2,6-bis(tert-butylthiomethyl)pyridine)EtOH] and [$NiCl_2$(2,6-bis(tert-butyl thiomethyl)pyridine)]

These complexes were prepared similarly to the Fe(II) complex by using $NiCl_2{\cdot}6H_2O$ (334.9 mg, 1.413 mmol).

Yellowish green crystals were obtained upon slow evaporation of the solvent under nitrogen. The crystals were collected, washed with ethanol and dried overnight under vacuum. Yield: 0.26 g (54%). FT-IR: ν(C=N), ν_{sym}(C–S), δ_{sym}(C–S), ν_{asym}(C–S), ν(M–N) and ν(M-S) are 1599, 1162, 880, 762, 575 and 430 cm^{-1}, respectively. Anal. calcd for $C_{15}H_{25}Cl_2NiNS_2.C_2H_5OH$: C, 44.44; H, 6.75; N, 3.05; S, 13.94. Found: C, 44.19; H, 6.30; N, 3.41; S, 14.34. The red complex was obtained by exposure of the green crystals to the air. Yield: 0.26 g (54%). FT-IR: ν(C=N), ν_{sym}(C–S), δ_{sym}(C–S), ν_{asym}(C–S), ν(M–N) and ν(M–S) are 1599, 1167, 876, 762, 575 and 430 cm^{-1}, respectively. Anal. calcd for $[NiCl_2(C_{15}H_{25}NS_2)]$: C, 43.61; H, 6.10; N, 3.39; S, 15.53. Found: C, 43.10; H, 6.16; N, 3.28; S, 15.02.

2.6. Synthesis of [$CuCl_2$(2,6-bis(tert-butylthiomethyl)pyridine)]

Again, the complex was synthesized as described for the Fe(II) complex, using $CuCl_2{\cdot}2H_2O$ (190 mg, 1.413 mmol). A deep green solid was obtained. Yield: 0.26 g (57%). FT-IR: ν(C=N), ν_{sym}(C–S), δ_{sym}(C–S), ν_{asym}(C–S), ν(M–N) and ν(M–S) are 1597, 1159, 876, 793, 554 and 430 cm^{-1}, respectively. Anal. calcd for $[CuCl_2(C_{15}H_{25}NS_2)]$: C, 43.11; H, 6.03; N, 3.35; S, 15.34. Found: C, 43.14; H, 6.01; N, 3.29; S, 15.23.

2.7. Synthesis of [$ZnBr_2$(2,6-bis(tert-butylthiomethyl)pyridine)]

The colorless compound was prepared as described above, using $ZnBr_2{\cdot}4H_2O$ (317.9 mg, 1.413 mmol). Yield: 0.67 g (75%). FT-IR: ν(C=N), ν_{sym}(C–S), δ_{sym}(C–S), ν_{asym}(C–S), ν(M–N) and ν(M–S) are 1599, 1163, 883, 766, 585 and 428 cm^{-1}, respectively. Anal. calcd. for $[ZnBr_2(C_{15}H_{25}NS_2)]$: C, 35.42; H, 4.95; N, 2.75; S, 12.61. Found: C, 35.29; H, 4.91; N, 2.65; S, 12.46. ^{1}H-NMR: δ = 7.95 (t, 3J(H,H) = 6.43 Hz, 1H, py), 7.54 (d, 3J(H,H) = 6.65 Hz, 2H, py), 4.33 (s, 4H,–CH_2–S) and 1.31 ppm (s, 18H,–$C(CH_3)_3$). ^{13}C {^{1}H}–NMR: δ = 157.93 (s, C1, py), 141.19 (s, C3, py), 123.63 (s, C2, py), 47.08 (s,–S–$C(CH_3)_3$), 34.91 (s,–CH_2–S) and 30.22 ppm (s,–$C(CH_3)_3$). Single crystals suitable for X-ray diffraction study of [$ZnBr_2$(2,6-bis(*tert*-butylthiomethyl)pyridine)] were obtained by slow evaporation of a dichloromethane solution.

2.7.1. Crystal structure determination of [$ZnBr_2$(2,6-bis(tert-butylthiomethyl)pyridine)]

The low-temperature dataset was collected on a STOE IPDS2 diffractometer with molybdenum radiation and corrected for absorption (numerical correction). The structure was solved by direct methods (SHELXS-97) [29] and refined with SHELXL-97 [30] by full-matrix least-squares refinement. All non-hydrogen atoms were refined anisotropically. For the hydrogen atoms, idealized atomic coordinates were generated using the HFIX instruction.

The crystals are systematically twinned (“racemic twins”), the twins being related through an inversion centre. Refinements were performed in both possible space groups. A TWIN and a BASF instruction were added in order to refine the ratio of the twin components (ratio of the two individuals of the twins: 59.2%:40.8%). The twin ratios calculated for both space groups exactly add up to one. The descriptions in both space groups are equivalent to each other; the only difference between the two space groups is that they contain four-fold screw axes of different handedness. The crystallographic data are given in Table 2, the atomic parameters and isotropic displacement parameters in Table 1S (space group *P*41212, No. 92) and Table 3S (space group *P*43212, No. 96), the anisotropic displacement parameters for the non-hydrogen atoms in Table 2S (space group *P*41212, No. 92) and Table 4S (space group *P*43212, No. 96).

3. Results and discussion

Tbtmp is an example of a tridentate ligand with two identical terminal coordination sites. The synthetic route to this (alkylthio) pyridine ligand is indicated in Scheme 1 and consists of the frequently employed preparation of sulfides by treating alkyl halides with salts of mercaptans.

Tbtmp has a yellowish color and was characterized by elemental analysis, infrared, ^{1}H-, and ^{13}C-NMR spectroscopy. The results of ^{1}H- and ^{13}C-NMR spectroscopies are in good agreement with the proposed structure. The ligand reacts easily at room temperature with salts of transition metals in the formal oxidation state 2+ to yield compounds with compositions $[M(L)X_2]$ (M = Fe, Cu, Ni, Co, X = Cl) and Zn (X = Br). The results of the elemental analysis of these stoichiometric complexes are in agreement with the proposed molecular formulae (Scheme 2). With Ni(II), two tbtmp complexes were obtained. The green crystals were found to present an octahedral geometry for Ni, according to the formula [$NiCl_2$(L)EtOH]. The red powder consists of $NiCl_2$(L) and has a trigonal bipyramidal structure. The ethanol-free compound forms when green crystals are exposed to air or nitrogen over a period of just a few hours. These complexes were isolated as mer isomers, similarly to $[Cu(dien)_2]^{2+}$ (dien = diethylene triamine) [26], $[Ni(dien)_2]^{2+}$ and $[Ni(dptn)_2]^{2+}$ (dptn = dipropylene-triamine) [28] and $[MX_2L]$ (M = Ni, Co, Cu, Zn and Cd, L = 2,6-bis(ethyl thiomethyl) pyridine, X = Cl, Br, SCN, NO_3), which were recently reported [22].

Since tbtmp has different coordination sites, infrared spectroscopy was considered as a useful technique to elucidate the way tbtmp bonds to the metal ions. Thus, infrared spectra of L and the effect of binding of Fe(II), Co(II), Ni(II), Cu(II) and Zn(II) ions on the vibration frequencies of the free ligand are discussed in detail in this paper. The IR spectrum of the ligand shows a sharp and strong band at 1589 cm^{-1}, which can be attributed to the vibration ν(C=N) of the pyridine ring [31]. When the ligand is coordinated to metal ions, this band shifts (8–11 cm^{-1})

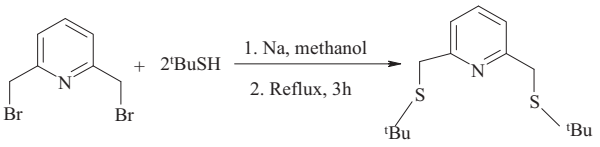

Scheme 1. Synthesis of the 2,6-bis(*tert*-butylthiomethyl)pyridine (tbtmp) ligand.

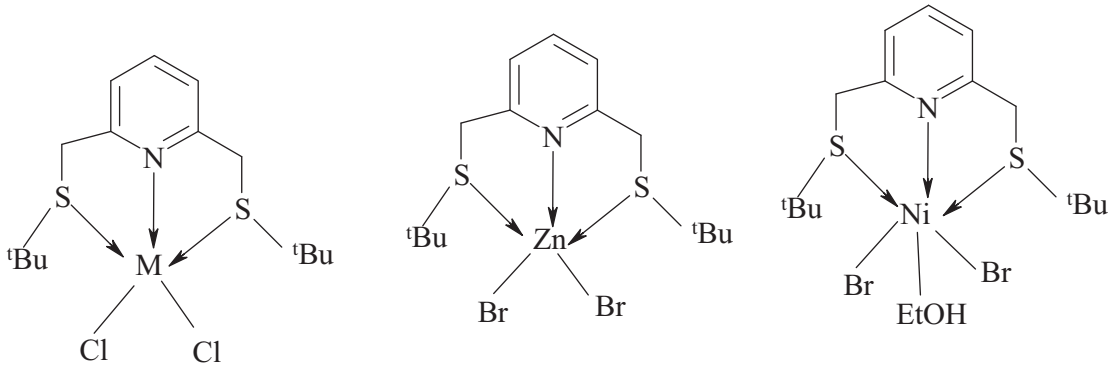

Scheme 2. Molecular formulae of the complexes (M = Fe(II), Co(II), Ni(II), Cu(II)).

to higher frequencies, indicating the involvement of the nitrogen atom of pyridine into the coordination scheme. The vibration mode ν(C–S-C) of the free ligand appears at 750 cm^{-1}. This band also shifts (12–43 cm^{-1}) to higher frequencies with the Fe(II), Ni(II), Cu(II) and Zn(II) complexes or to a lower frequency (shifted by 37 cm^{-1}) with the Co(II) complex. This can be explained by the involvement in the complex formation of the sulfur atom of the *tert*-butyl-sulfur-methylene-pyridine-methylene-sulfur chain. The bands observed for the complexes at 554–575 and 428–457 cm^{-1} are attributed to ν(M–N) [31] and ν(M–S) [32], respectively. The infrared spectra indicate that tbtmp behaves as a neutral tridentate (SNS) ligand. The coordinating sites are the pyridine *N* atom and two *S* atoms.

Reactions of tbtmp and transition metals in the oxidation state 2+ were carried out in ethanol. Trigonal bipyramidal metal complexes were obtained with the three available coordinating positions occupied by the unaltered NS_2 ligand and the other two positions occupied by halide anions. A comparison of the ^{1}H-NMR spectrum of the ligand [33] with that of its Zn(II) complex shows a downfield shift from δ = 7.58 (t, 1H, py) and 7.29 ppm (d, 2H, py) (in the ratio 1:2) to δ = 7.95 (t, 1H, py) and 7.54 ppm (d, 2H, py) (in the same ratio 1:2) for the two signals of the pyridine moiety. The methylene and *tert*-butyl groups adjacent to the sulfur atom shift from δ = 3.91 (s, 4H,–CH_2) and 1.34 ppm (s, 18H,–$C(CH_3)_3$), respectively, to δ = 4.33 and 1.31 ppm as a result of coordination of the sulfur atom to the Zn(II) metal.

The ^{13}C-NMR spectrum of the free ligand is the same as for its Zn(II) complex, but with a chemical shift in the resonances of the carbon atoms. The resonances of the carbon atoms of the pyridine moiety at 158.65, 136.99 and 121.52 ppm are shifted to 157.93, 141.19 and 123.63 ppm in the Zn complex. Also the methylene (–CH_2–S), the tertiary carbon atom of the *tert*-butyl group (–S–$C(CH_3)_3$) and the methyl group of the *tert*-butyl branch (–S–$C(CH_3)_3$) resonances are shifted from 43.09, 35.55 and 30.99 ppm, respectively, in the free ligand, to 47.08, 34.91 and 30.22 ppm, in the coordinating ligand. It also appears that the C3 atom of the pyridine molecule and the methylene carbon atoms are more affected by complexation than other carbon atoms of the ligand.

In the present investigation, the weight loss for each chelate ligand was calculated within the corresponding temperature ranges given in Table 1. The TG curve of $[CuCl_2(C_{15}H_{25}NS_2)]$ exhibits an estimated mass loss of 13.23% (calcd 13.39%) within the temperature range between 30 and 180 °C, which may be attributed to the liberation of a C_5H_6N molecule. Between 180 and 800 °C, $C_{10}H_{19}Cl_2S$ is subtracted under decomposition into 2HCl and $C_6H_{17}S$, the mass loss was estimated at 45.59% (calcd 46.41%). The residue consists of CuS and carbon and was estimated at 34.98% (calcd 34.33%).

The TG curve of $[NiCl_2(C_{15}H_{25}NS_2)]$ shows three decomposition steps within the temperature range from

Table 1
Data from thermal gravimetry (TG) and differential thermal analysis (DTA) of tbtmp metal complexes.

Complex	TG range (°C)	Peak temp. in DTA (°C)	Mass loss	Total mass loss	Assignment	Residue estim (calcd)%
			Estim (Calcd) %			
$[CuCl_2(C_{15}H_{25}NS_2)]$	30–180	123(+), 144(−)	19.43 (19.14)		Loss of C_5H_6N	CuS + 4C
	180–275	182(+), 216(−)	37.46 (37.68)		Loss of HCl and $C_6H_{17}S$	34.98 (34.33%)
	275–800	500(+)	8.23 (8.73)	65.12 (65.55)	Loss of HCl	
$[NiCl_2(C_{15}H_{25}NS_2)]$	30–275	201(+), 227(−)	37.98 (38.74)		Loss of C_3H_5NS and 2HCl	
	275–420	289(+), 333(−)	7.25 (6.77)		Loss of C_2H_4	NiS + 3C
	420–660	414(+), 470(−)	22.78 (23.24)	68.01 (68.75)	Loss of C_7H_{12}	31.68 (30.75%)
$[ZnBr_2(C_{15}H_{25}NS_2)]$	50–280	190(+), 228(−)	32.75 (33.99)		Loss of C_6H_6N and HBr	
	290–675	600(−), 380(+)	34.42 (35.75)		Loss of HBr and $2H_2S$, C_2H_6 and $1.5H_2$	ZnS + 5C
	675–800	800(−)	5.75 (5.50)	73.02 (73.86)	Loss of C_2H_4	26.82 (26.97%)

tbtmp: 2,6-bis(*tert*-butylthiomethyl)pyridine.

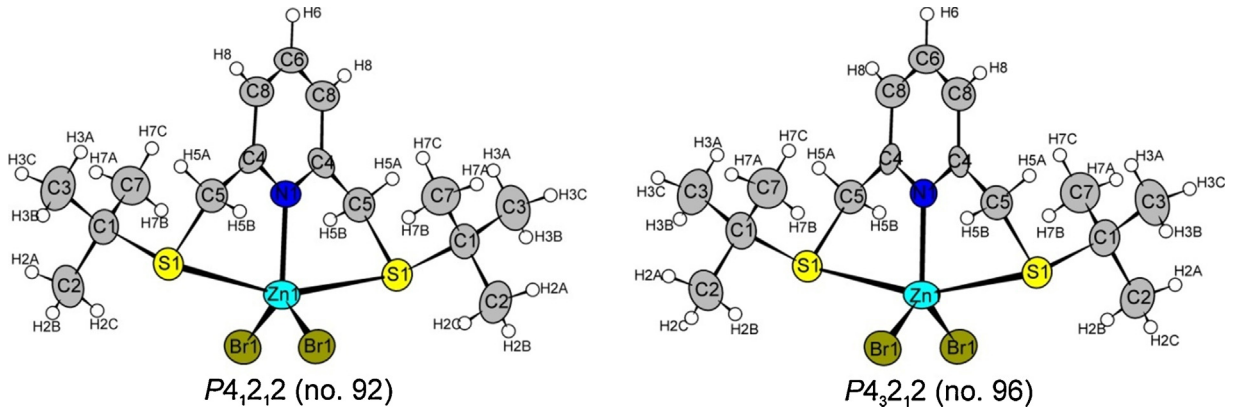

Fig. 1. (Color online.) Molecular structures of $C_{15}H_{25}ZnS_2NBr_2$ in the two enantiomorphous space groups. The displacement parameters are drawn at an 80% probability level (light blue: Zn; dark blue: N; grey: C; yellow: S; olive: Br).

30 to 660 °C. The first step of decomposition that occurs from 30 to 275 °C corresponds to the loss of C_3H_5NS and two HCl molecules with a mass loss of 37.88% (calcd 38.74%). In the second stage (275–420 °C), the weight loss may be attributed to the loss of C_2H_4 (observed 7%, calcd 6.77%). The subsequent steps (420–660 °C) correspond to the removal of C_7H_8, leaving nickel sulfide and carbon as residues.

The TG curve of $[ZnBr_2(C_{15}H_{25}NS_2)]$ shows three decomposition steps within the temperature range from 50 to 800 °C. Between 50 and 280 °C and between 290 and 675 °C, C_6H_6N, two molecules of HBr per formula, two molecules of H_2S, C_2H_6 and 1.5 equivalents of H_2 are subtracted. Finally, a loss of C_2H_4 (observed 5.75%, calcd 5.50%) is observed. The appearance of many exothermic and endothermic peaks in the DTA (Table 1) can be attributed to the loss of the bromide and chloride anions and ligand molecules.

The $C_{15}H_{25}Br_2NS_2Zn$ molecule is chiral. The compound crystallises in the tetragonal crystal system in the chiral space groups *P*41212 (No. 92) and *P*43212 (No. 96), respectively. In Fig. 1, both molecular structures are shown, indicating that the molecules are mirror images of each other. The crystal structure data are listed in (Table 2, Tables 1S–4S).

The unit cell of the compound is shown in Fig. 2. Additional data has been deposited under CCDC Nos. 817449 and 817450 [34].

The interest towards transition-metal complexes containing a NS-donor was triggered by a wish to obtain metal-based drugs with elevated biological activity in combination with reduced toxicity. The data obtained for the metal complexes described above show that some of them have the capacity of inhibiting the metabolic growth of the investigated bacteria and fungi. The activities of all complexes tested may be explained on the basis of chelation theory. Chelation reduces the polarity of the metal atom mainly because it partially shares its positive charge with the donor groups and possible π electron delocalization takes place within the whole chelate ring. Also, chelation increases the lipophilic nature of the central atom, which subsequently favors its permeation through the lipid layer of the cell membrane. It was described in the literature that lipophilic side chains may influence the interaction between molecules to lead to a degradation of the bacteria cellular membrane and the leakage of cellular contents [35].

In the present study, antibacterial activities of Fe(III), Co(II), Ni(II) and Cu(II) complexes of tbtmp were compared to standard drugs (Amikacin and Ketokonazole) by screening with the agar-cup method. DMSO was used as

Table 2
Crystallographic data of $C_{15}H_{25}Br_2NS_2Zn$.

Formula	$C_{15}H_{25}Br_2NS_2Zn$	
Molecular weight/gmol^{-1}	508.67	
Crystallite size/mm^3	$0.312 \times 0.303 \times 0.069$	
Space group	$P4_12_12$ (No. 92)	$P4_32_12$ (No. 96)
Crystal system	Tetragonal	
Formula units	4	
Temperature/K	153.15	
a/pm	947.2(1)	
c/pm	2265.2(5)	
$V/10^6$pm^3	2032.24	
Wave length/pm	71.073	
Diffractometer	IPDS-II	
Number of measured reflections	5923	
Independent reflections	2829	
Refined parameters	104	
Flack parameter	Racemic twin, BASF 0.59208	Racemic twin, BASF 0.40792
$\delta_{min}/\delta_{max}$(e/$10^6$pm^3)	0.68/−0.57	0.67/−0.50
R_{int}	0.0463	0.0463
R_1 ($F_O > 4\sigma$)	0.0255	0.0255
R_1/all reflections	0.0754	0.0754
wR_2	0.0394	0.0394
GOF	0.428	0.427

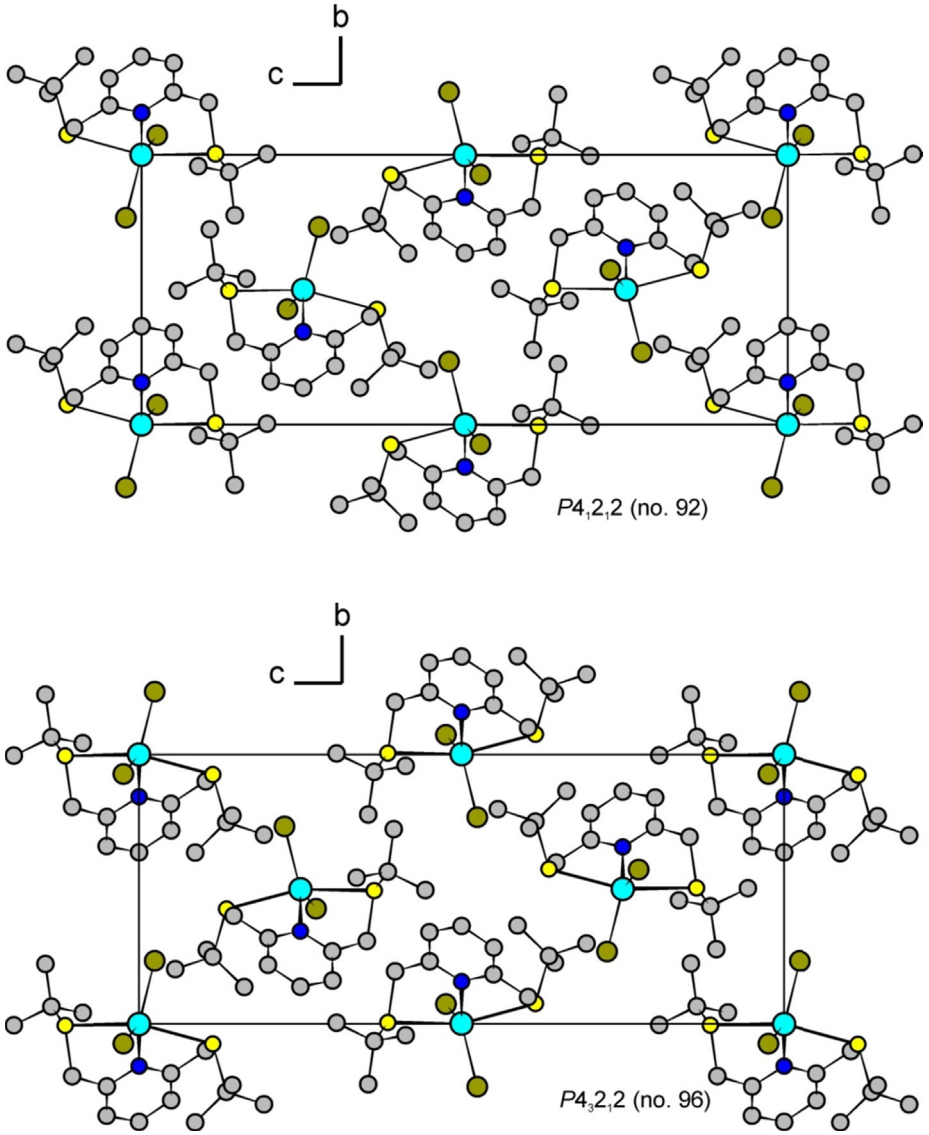

Fig. 2. (Color online.) Unit cell of $C_{15}H_{25}ZnS_2NBr_2$ (light blue: Zn; dark blue: N; grey: C; yellow: S; olive: Br).

the solvent at a complex concentration of 50 μg/mL. The chemicals were checked against gram positive bacteria *B. subtilis* and gram negative bacteria *Escherichia coli* (Table 3). Diameters of inhibition zones of the standard drug Amikacin against gram positive bacteria [36] (*B. subtilis*) and gram negative bacteria (*E. coli*) were found to be 6 mm, while the corresponding values for metal complexes in identical conditions were established to be 27, 24, 14, and 18 mm, respectively with G+ bacteria, 25, 26, 14 and 16 mm, with G− bacteria (Table 3). Fe(III), Co(II), Ni(II) and Cu(II) complexes were also screened for their antifungal activities against two fungi (*Aspergillus flavus* and *Candida albicans*). The results (Table 3) show that most of the complexes exhibit almost no activity with *A. flavus*, but high activity with *C. albicans*. Only the Co(II) complex has antifungal activity against *A. flavus*. For *C. albicans*, it is clear from (Table 3) that the antifungal activities of the complexes follow the order Co(II) > Cu(II) > Fe(III) > Ni(II).

Table 3
Biological activity of the ligand and of its metal complexes tested using the diffusion agar technique. The inhibition zone diameter is given as mm/mg sample (solvent: DMSO).

Metal complexes	Fungus		G(−)	G(+)
	Aspergillus flavus	*Candida albicans*	*Escherichia coli*	*B. subtilis*
$[FeCl_2(C_{15}H_{25}NS_2)]$	0.0	14	25	27
$[CoCl_2(C_{15}H_{25}NS_2)]$	14	21	26	24
$[NiCl_2(C_{15}H_{25}NS_2)]$	0.0	12	14	14
$[CuCl_2(C_{15}H_{25}NS_2)]$	0.0	20	16	18
Amikacin	–	–	6	6
Ketokonazole	9	9	–	–

Coming to *B. subtilis* (G+ bacteria), it becomes obvious that the antibacterial activity follow the order Co(II) > Cu(II) > Fe(III) > Ni(II), although the inhibition with Fe(III) remains incomplete. Finally, using *E. coli* (G− bacteria), we found that antibacterial activity follows the order Co(II) > Fe(III) > Cu(II) > Ni(II).

Also, we tried to investigate the inhibition on a breast cancer cell line (MCF7) by the Zn(II) Cu(II), Ni(II) and Fe(III) complexes. The results showed an inhibition of less than 70%, decreasing from Zn(II) to Cu(II), Ni(II) and Fe(III).

4. Conclusions

The tbtmp ligand was synthesized and coordinated to several transition-metal ions. It was found to be meridionally coordinated with coordination number five for the metal ions. Only one complex with a solvent molecule as an additional ligand had metal ions that were facially coordinated pseudo-octahedrally. The infrared spectra confirmed that tbtmp binds to the metal ions via the pyridine nitrogen and two sulfur atoms. The metal complexes show biological activities higher than the parent ligand but lower than the standard compounds amphotericin and tetracycline.

Acknowledgements

G.G. Mohamed thanks the Spanish Ministry of Education for financial support. This work was partially supported by contracts PL972004 (European Union) and AMB1999-1810-CE (Spain).

Appendix A. Supplementary data

Supplementary data associated with this article can be found, in the online version, at http://dx.doi.org/10.1016/j.crci.2014.10.004.

References

[1] J.P. Collman, L.S. Hegedus, J.R. Norton, R.G. Finke, Principles and Applications of Organotransition Metal Chemistry, 2nd edition, University Science, Mill Valley, CA, 1987.
[2] (a) P. Margl, J.C. Lohrenz, T. Ziegler, P.E. Blochl, J. Am. Chem. Soc. 118 (1996) 4434;
(b) R.H. Grubbs, G.W. Coates, Acc. Chem. Res. 29 (1996) 85.
[3] (a) H.D. Empsall, E.M. Hyde, B.L. Shaw, M.F. Uttley, J. Chem. Soc., Dalton Trans. 20 (1976) 2069;
(b) J. Halpern, Pure Appl. Chem. 73 (2001) 209;
(c) J.A. Loch, R.H. Crabtree, Pure Appl. Chem. 73 (2001) 119;
(d) D. Morales-Morales, R. Redon, C. Yung, C.M. Jensen, Inorg. Chim. Acta 357 (2004) 2953;
(e) A. Naghipour, S.J. Sabounchei, D. Morales-Morales, S. Hernandez Ortega, C.M. Jensen, J. Organomet. Chem. 689 (2004) 2494;
(f) H.P. Dijkstra, M.Q. Slagt, A. McDonal, C.A. Kruithof, R. Kreiter, A.M. Mills, M. Lutz, A.L. Spek, W. Klopper, G. Klink, G. Koten, Eur. J. Inorg. Chem. 2003 (2003) 830.
[4] P. Bhattacharya, J.A. Krause, H. Guan, Organometallics 30 (2011) 4720.
[5] A. Sattler, G. Parkin, J. Am. Chem. Soc. 134 (2012) 2355.
[6] R. Manikandan, P. Viswnathamurthi, Spectrochim. Acta A 97 (2012) 864.
[7] R. Ramachandran, P. Viswanathamurthi, Spectrochim. Acta A 103 (2013) 53.
[8] A. Khalid, S. Yacoob, A. Zeeshan, K. Ilia, G. Sandro, D. Robbert, Organometallics 30 (2011) 4159.
[9] M. Page, J. Wagler, B. Messerle, Organometallics 29 (2010) 3790.
[10] (a) M. Albrecht, M. Schlupp, J. Bargon, G. Van Koten, Chem. Commun. 18 (2001) 1874;
(b) C. Seward, W.L. Jia, R.Y. Wang, S. Wang, Inorg. Chem. 43 (2004) 978.
[11] (a) M. Gandelman, L. Konstantinovski, Chem. Eur. J. 9 (2003) 2595;
(b) E. Poverenov, G. Leitus, L.J.W. Shimon, Organometallics 24 (2005) 5937.
[12] M. Albrecht, M. Lutz, A. Spek, G. Van Koten, Nature 406 (2000) 970.
[13] P. Steenwinkel, D.M. Grove, N. Veldman, A.L. Spek, G. Van Koten, Organometallics 17 (1998) 5647.
[14] P. Steenwinkel, H. Kooijman, W. Smeets, A. Spek, D. Grove, G. Koten, Organometallics 17 (1998) 5411.
[15] (a) P.L. Alsters, P.J. Baesjou, M.D. Janssen, H. Kooijman, A. Sicherer-Roetman, A.L. Spek, G. Koten, Organometallics 11 (1992) 4124;
(b) G. Rodriguez, M. Albrecht, J. Schoenmaker, A. Ford, M. Lutz, A. Spek, G. Koten, J. Am. Chem. Soc. 124 (2002) 5127;
(c) C. Amijs, A. Berger, F. Soulimani, T. Visser, G. Klink, M. Lutz, A. Spek, G. Koten, Inorg. Chem. 44 (2005) 6567.
[16] M. Albrecht, G. Koten, Angew. Chem., Int. Ed. 113 (2001) 3750.
[17] W. Huck, L. Prins, R. Fokkens, N. Nibbering, F. Veggel, D. Reinhoudt, J. Am. Chem. Soc. 120 (1998) 6240.
[18] (a) J. Pollino, M. Weck, Synthesis 9 (2002) 1277;
(b) J. Pollino, L. Stubbs, M. Weck, J. Am. Chem. Soc. 126 (2004) 563;
(c) J. Pollino, M. Weck, Chem. Soc. Rev. 34 (2005) 193.
[19] A. Canty, G. Koten, Acc. Chem. Res. 28 (1995) 28406.
[20] D. Barker, J. Lehn, J. Rimmer, J. Chem. Soc., Dalton Trans. 7 (1985) 1517.
[21] F. Teixidor, L. Escriche, J. Casabo, E. Molins, C. Miravitlles, Inorg. Chem. 25 (1986) 4060.
[22] L. Escriche, M. Sanz, J. Casabo, F. Teixidor, E. Molins, C. Miravitlles, J. Chem. Soc., Dalton Trans. 9 (1989) 1739.
[23] L. Canovese, F. Visentin, G. Chessa, P. Uguagliati, C. Levi, A. Dolmella, Organometallics 24 (2005) 5537.
[24] F. Teixidor, L. Escriche, I. Rodriguez, J. Casabo, J. Rius, E. Molins, B. Martinez, C. Miravitlles, J. Chem. Soc., Dalton Trans. 7 (1989) 1381.
[25] L. Canovese, F. Visentin, G. Chessa, G. Gardenal, P. Uguagliati, J. Organomet. Chem. 622 (2001) 155.
[26] C. Vinas, P. Angles, G. Sanchez, N. Lucena, F. Teixidor, L. Escriche, J. Casabo, J. Piniella, J. Alvarez-Larena, R. Kivekas, R. Sillanpa, Inorg. Chem. 37 (1998) 701.
[27] J. Casabo, L. Escriche, S. Alegret, C. Jaime, C. Perez-Jimenez, L. Mestres, J. Rius, E. Molins, C. Miravitlles, F. Teixidor, Inorg. Chem. 30 (1991) 1893.
[28] W. Offermann, F. Vogtle, Synthesis 4 (1977) 272.
[29] G.M. Sheldrick, SHELXS-97, Program for Solution of Crystal Structures, University of Göttingen, Germany, 1997.
[30] G.M. Sheldrick, SHELXS-97, Program for Refinement of Crystal Structures, University of Göttingen, Germany, 1997.
[31] G. Mohamed, Spectrochim. Acta A 64 (2006) 188.
[32] G. Hogarth, K. Holman, A. Pateman, A. Sella, W. Jonathan, Dalton Trans. (2005) 2688.
[33] L. Canovese, G. Chessa, C. Santo, F. Visentin, P. Uguagliati, Organometallics 21 (2002) 4342.
[34] CCDC 817449 and CCDC 817450 contain the supplementary crystallographic data. These data can be obtained free of charge via www.ccdc.cam.ac.uk/data_request/cif, or by emailing data_request@ccdc.cam.ac.uk, or by contacting The Cambridge Crystallographic Data Centre, 12, Union Road, Cambridge CBZ 1 EZ, UK, fax +44 1223 336033.
[35] D. Demberelnyamba, K. Kim, S. Choi, S. Park, H. Lee, C. Kim, I. Yoo, Bioorg. Med. Chem. 12 (2004) 853.
[36] K. Ram, K. Agarwal, L. Singh, Bioinorg. Chem. Appl. 2006 (2006) 29234.